Electronic Supplementary Material (ESI) for ChemComm.


# Supporting Information

## Large-scale production of chiral nematic microspheres

Jiaqi Yu,[a] Zhixiang Wang,[a] Sirui Chen,[a] Qiongya Li,[b] Yi Qian,[a] Hao Wang,[a] Yuxiao Huang,[a] Fusheng Zhang*[ab] and Guangyan Qing*[ab]

[a] Hubei Key Laboratory of Biomass Fibers and Eco-dyeing & Finishing, College of Chemistry and Chemical Engineering, Wuhan Textile University, Wuhan 430200 P. R. China

[b] CAS Key Laboratory of Separation Science for Analytical Chemistry, Dalian Institute of Chemical Physics, Chinese Academy of Sciences, Dalian 116023, P. R. China

E-mail: fszhang@wtu.edu.cn, qinggy@dicp.ac.cn

## 1. Materials and instruments

All reagents and solvents without further purification including tetramethyl orthosilicate (TMOS, 98%), Span 80 (≥99.5%), and *n*-hexadecane (99%), were purchased from Sinopharm Chemical Reagent Co. CNC aqueous suspension was prepared as in the published procedure.[1] Subsequently, a concentration method was employed to adjust the mass concentration of CNCs to 6.0 wt% using a rotary evaporator. Double deionized water (18.2 MΩ·cm$^{-1}$) was used for all the experiments.

Zeta potential was measured using a Zetasizer ZS90 from Malvern Instruments. Polarized optical microscopy images were captured in reflection with crossed polarizers using an Olympus BX53 microscope to detect the chiral nematic phase of the microdroplets, solid particles, and other derivatization materials. Scanning electron microscopy (SEM) samples were mounted on aluminum stubs using conductive carbon tape, and their images were collected using a Carl Zeiss electron microscope with ORION NanoFab. The slicing experiment was carried out using a Leica UC7FC7. Circular dichroism (CD) spectra were recorded using a BioTools MOS450 spectropolarimeter. Thermogravimetric analysis (TGA) was performed on a Diamond TG/DTA Instrument (STA 449 F3, Netzsch) up to 800°C with a heating rate of 10.0 °C·min$^{-1}$ under air atmosphere. Nitrogen adsorption−desorption studies were conducted by using a QUADRASORB SI analyzer. Prior to analysis, samples were degassed under vacuum for 4 hours.

## 2. Preparation of CNC−silica microdroplets and solid microspheres

TMOS was added dropwise into the CNC suspension, and the mixture was stirred for 2 hours at room temperature to prepare the aqueous phase. The oil phase consisted of *n*-hexadecane containing 1.0 wt% Span 80 and was stirred continuously in a dry beaker. The syringe and direct membrane emulsifier ($\Phi$=20 μm, SPG DC20U) were connected using a Luer extension tube. Then the aqueous

phase was injected into the oil phase using a syringe pump (ISPLab10, Baoding Shenchen Pump Industry Co., Ltd) at a flow rate of 0.75 mL·h$^{-1}$. At the oil-water interface, shear forces facilitate the formation of water-in-oil droplets. Finally, drying and collecting the CNC-silica composite spheres in an oven at 40°C.

**3. Preparation of chiral nematic mesoporous carbon and silica microparticles.**

The preparation of chiral nematic mesoporous carbon spheres involved the pyrolysis of cellulose.[2] Initially, CNC-silica composite spheres were subjected to a gradual heating process at a rate of 2 °C·min$^{-1}$, until reaching a temperature of 100°C. This step was carried out under a flowing nitrogen atmosphere and lasted for 2 hours. Subsequently, the composite spheres were further heated to 900°C for a duration of 6 hours, using the same heating rate. After allowing the spheres to cool down to room temperature, they were soaked in a 2.0 M sodium hydroxide solution at a temperature of 90°C for 4 hours. The resulting microspheres were then filtered and thoroughly rinsed with water, followed by drying at room temperature. This procedure ultimately yielded chiral mesoporous carbon spheres.

The preparation of chiral nematic mesoporous silica spheres was conducted using the mentioned method.[1] CNC-silica composite spheres were directly calcined in a muffle furnace at a rate of 2 °C·min$^{-1}$ in air. The temperature was raised to 100°C and maintained for 2 hours, then further heated to 540°C and maintained for 6 hours. After cooling to room temperature, chiral ordered mesoporous silica spheres were recovered.

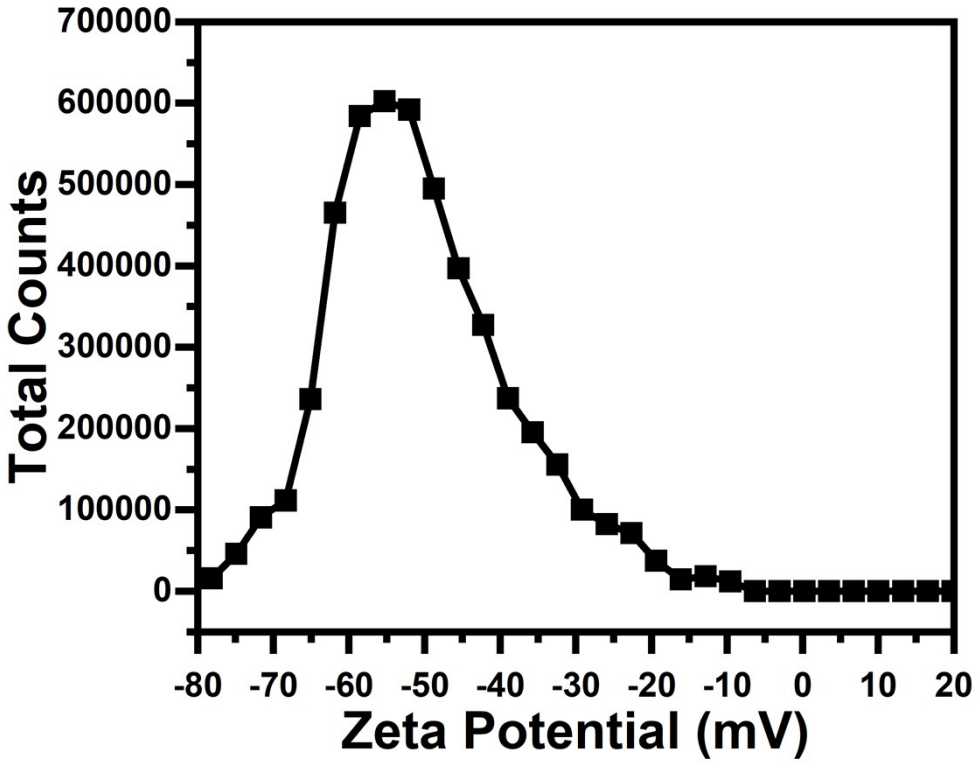


**Figure S1.** Zeta-potential distribution of CNCs with the concentration of 6.0 wt%.

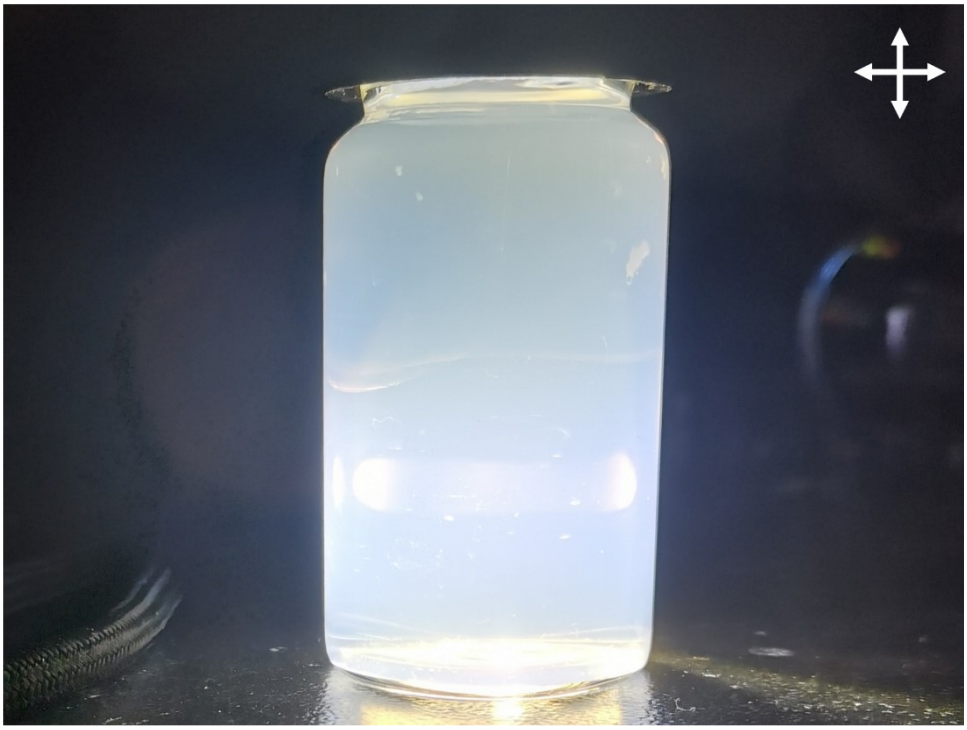

**Figure S2.** CNC/TMOS suspension in water solvent viewed under crossed polarizers.

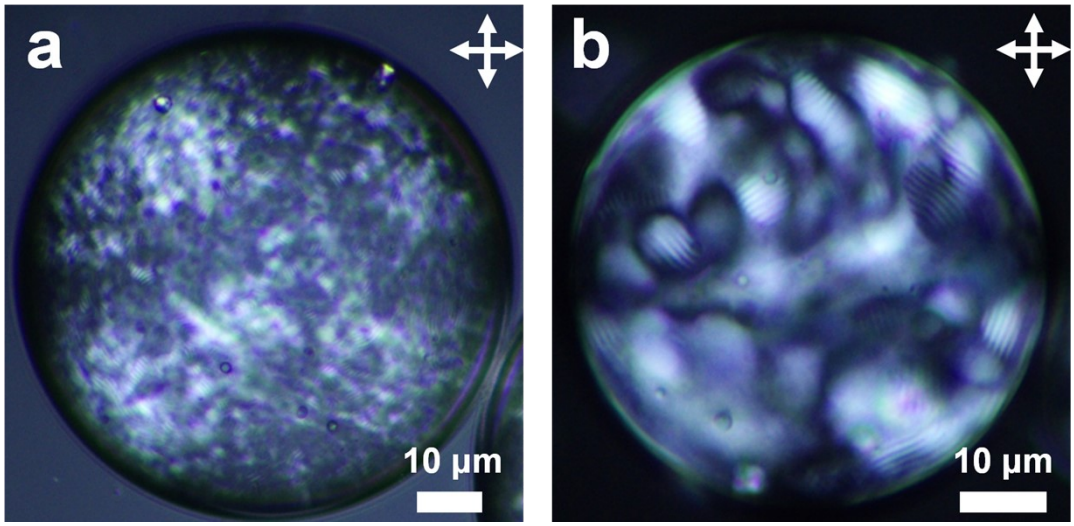


**Figure S3.** POM images of microdroplets in different drying states. The initial microdroplets (a), corresponding to microdroplets after 0.5 hours of drying (b).

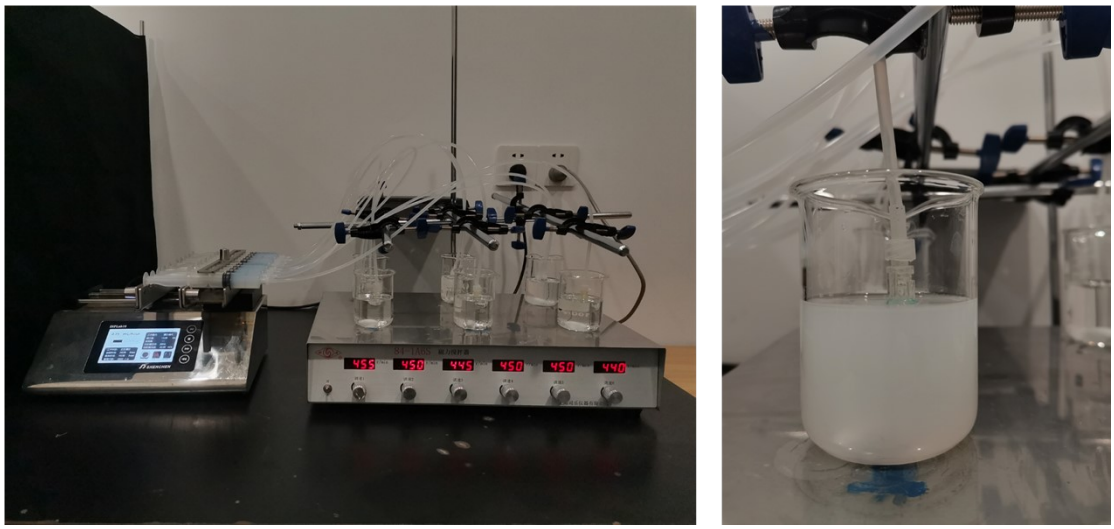

**Figure S4.** Photograph of the setup for producing microdroplets using a 10-channel syringe pump.

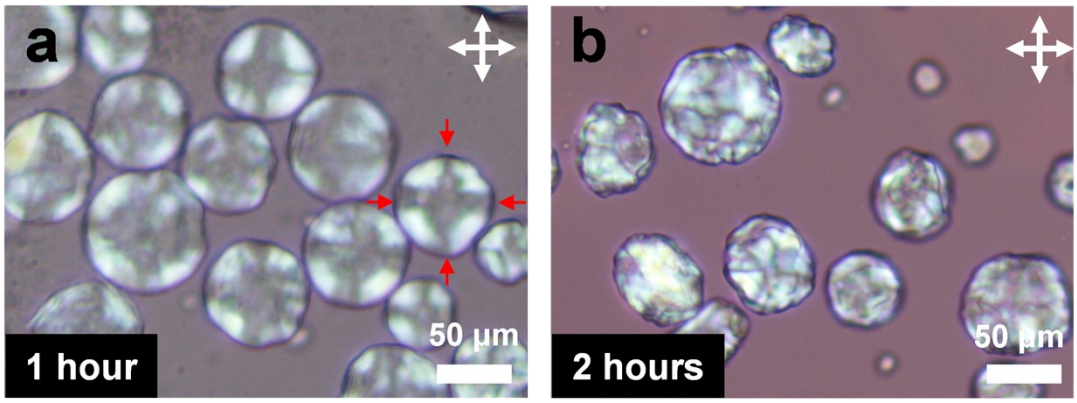


**Figure S5**. POM images of microdroplets in different drying states at higher magnification. Initial microdroplets (a), and microdroplets after 2 hours of drying (b).

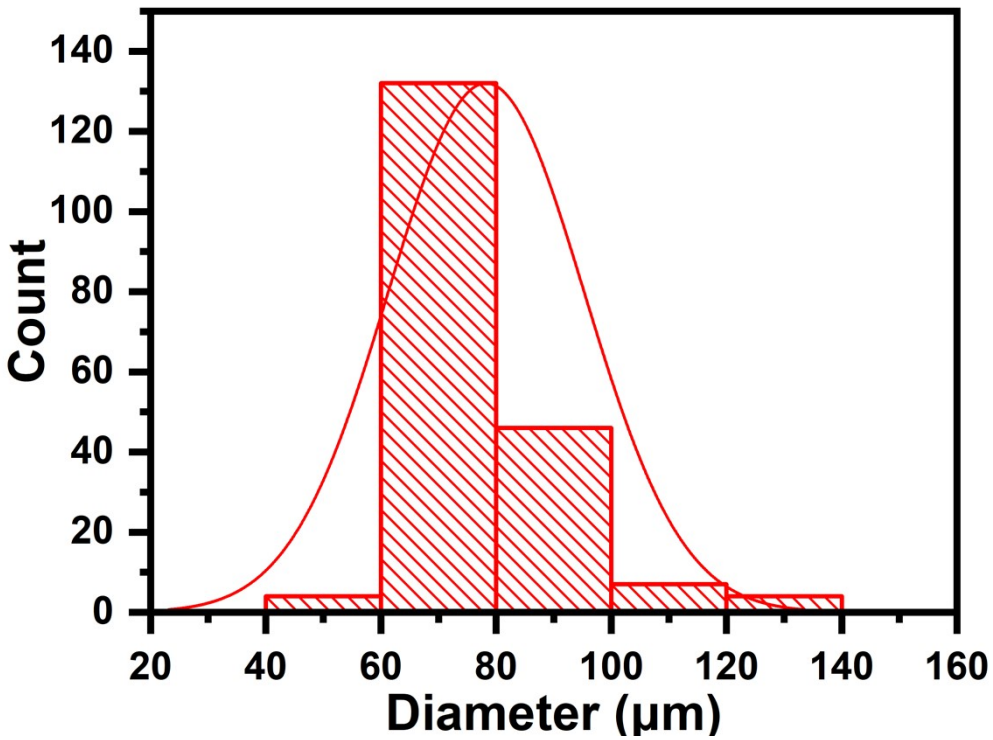


**Figure S6.** Particle size distribution of microdroplets.

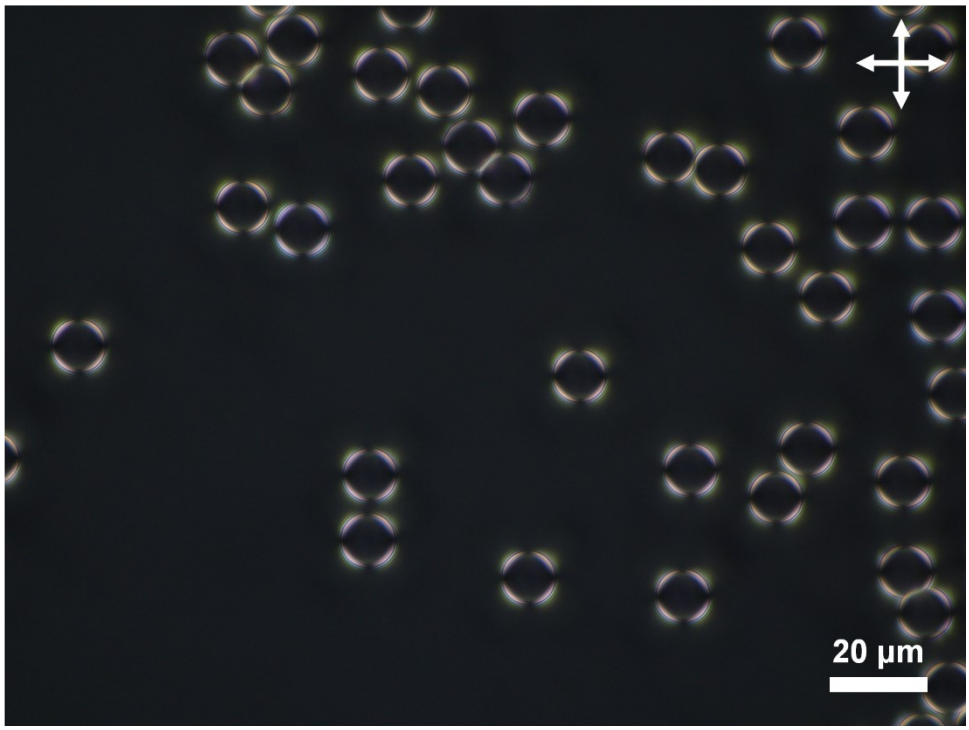


**Figure S7.** POM image of commercial silica particles under crossed polarizers.

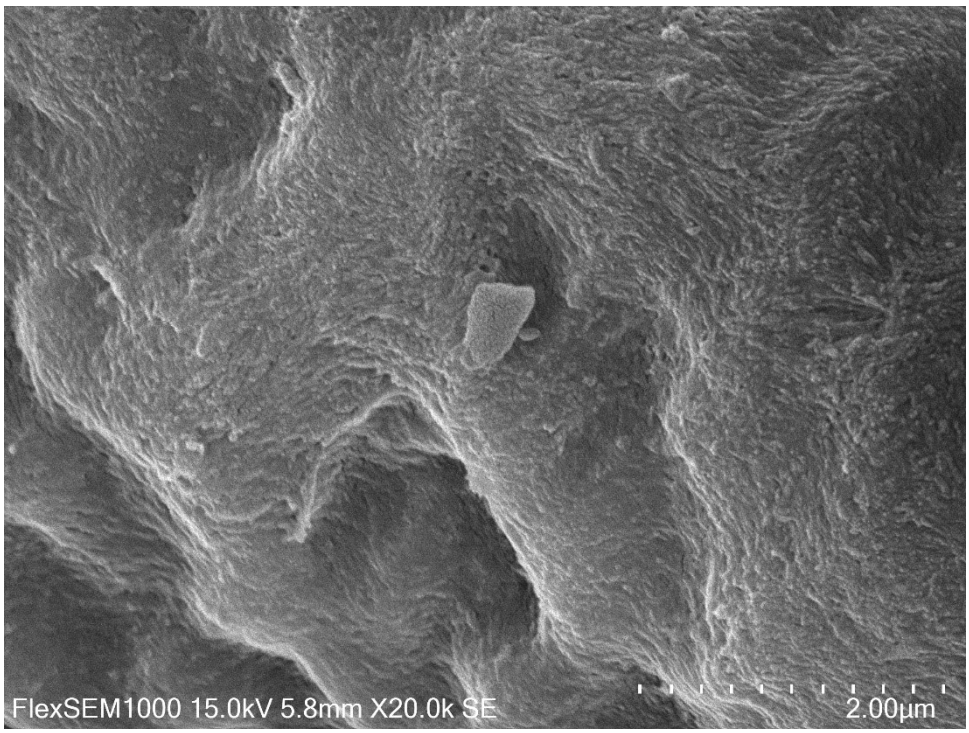


**Figure S8.** SEM image of a depression in the CNS surface.

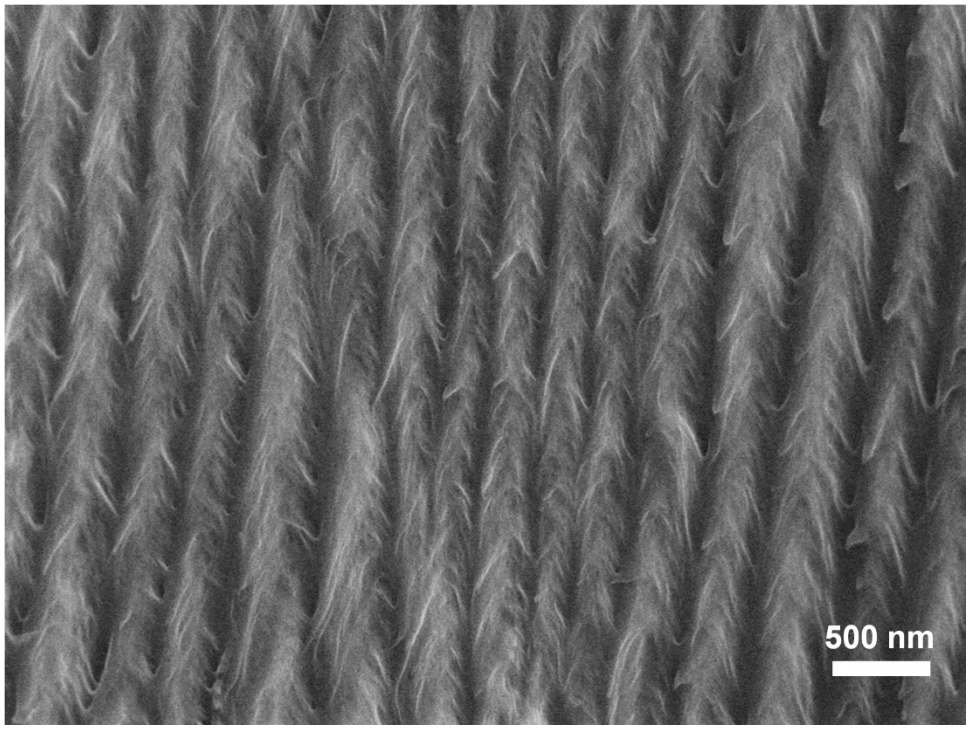


**Figure S9.** Cross-sectional SEM image of a CNC film with a continuous multilayer structure.

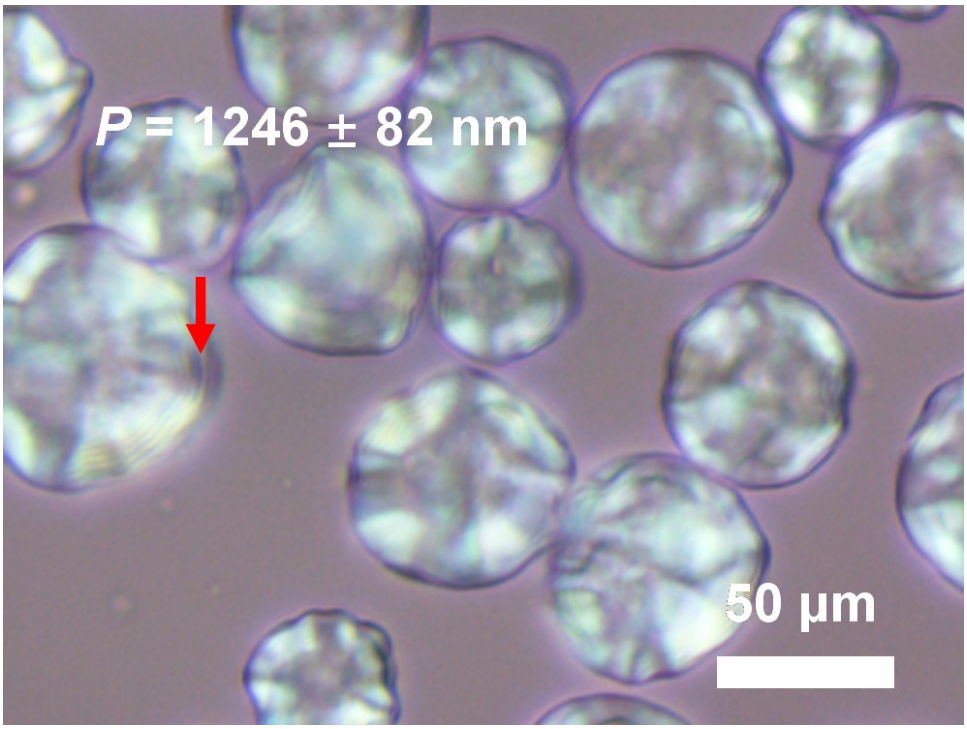


**Figure S10.** Images of microdroplets with Frank-Price texture after 1 hour of drying.

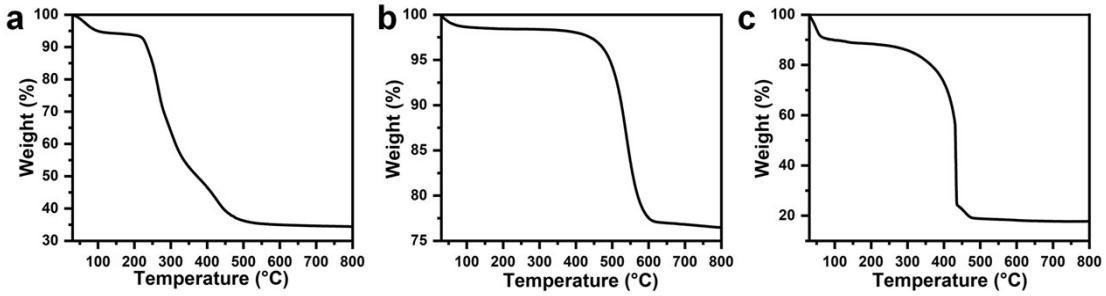


**Figure S11.** Thermogravimetric analysis (10 °C·min$^{-1}$, air) of CNC−silica composite materials (a), carbon−$SiO_2$ composite (b), and mesoporous carbon (c).

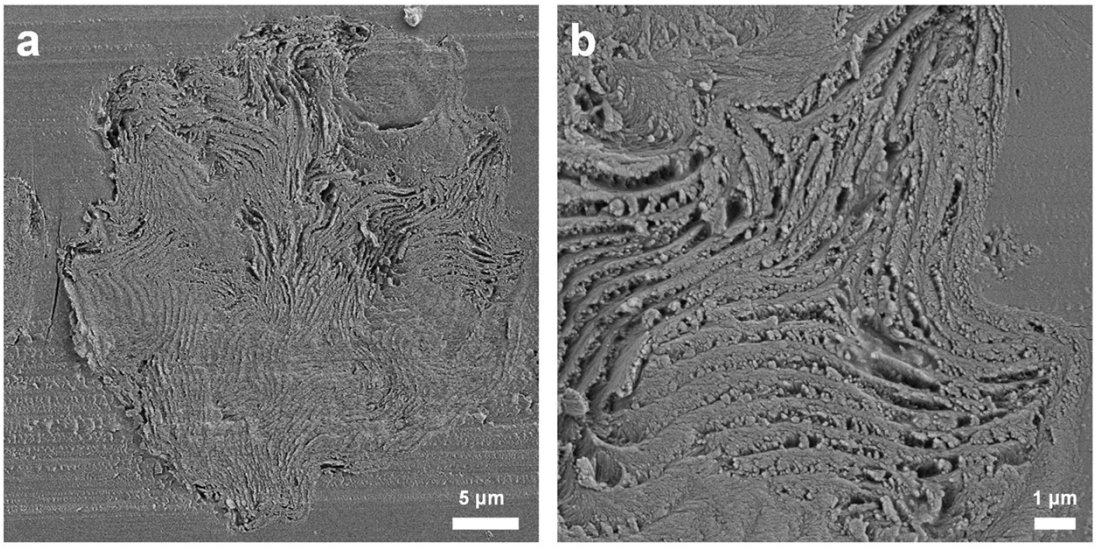


**Figure S12.** Cross-section SEM image of carbon spheres containing multilayer structures.

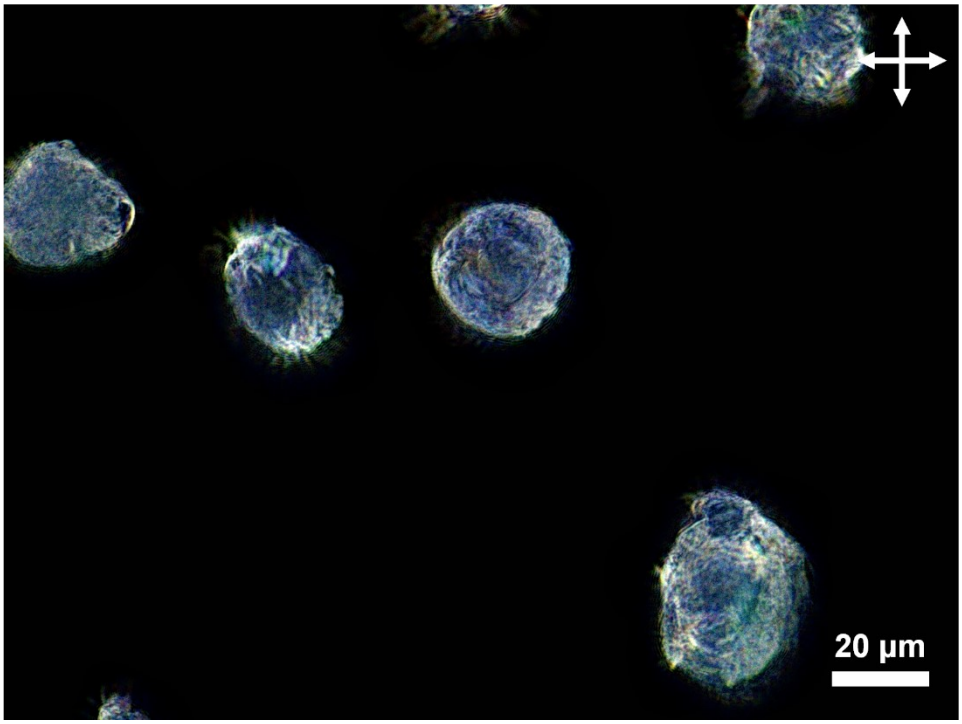


**Figure S13.** POM image of chiral nematic mesoporous silica spheres, showing strong birefringence.

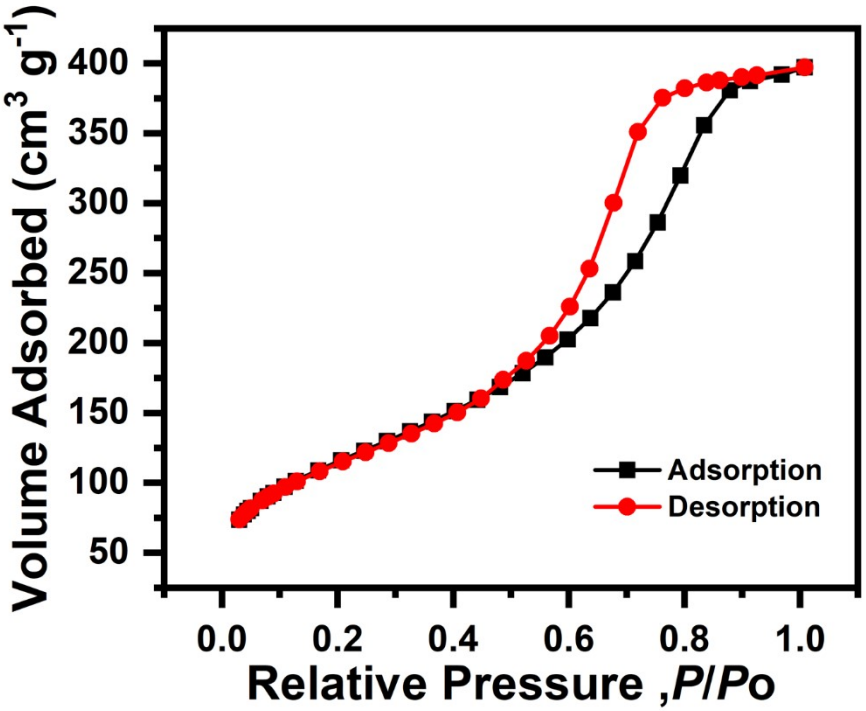


**Figure S14.** Nitrogen adsorption−desorption isotherms of chiral nematic mesoporous silica spheres.

**Table S1.** Nitrogen adsorption−desorption measurements for the CNS, and chiral nematic mesoporous carbon spheres (CNMC), chiral nematic mesoporous silica spheres (CNMS).

| Samples | BET surface area ($m^2 \cdot g^{-1}$) | pore volume ($cm^3 \cdot g^{-1}$) | BJH pore diameter (nm) |
|---|---|---|---|
| CNS | 310 ± 22 | 0.21 ± 0.11 | − |
| CNMC | 1438 ± 10 | 1.12 ± 0.06 | 3.2 ± 0.1 |
| CNMS | 418 ± 13 | 0.58 ± 0.01 | 5.3 ± 0.2 |

## Reference


1 F. Zhang, D. Wang, H. Qin, L. Feng, X. Liang and G. Qing, *ACS Appl. Mater. Interfaces*, 2019, **11**, 13114.

2 K. E. Shopsowitz, W. Y. Hamad and M. J. MacLachlan, *Angew. Chem. Int. Ed.*, 2011, **123**, 11183.